



Article

# Arsenic, Iron, and Manganese Adsorption in Single and Ternary Heavy Metal Solution Systems by Bamboo-Derived Biochars

Anawat Pinisakul <sup>1</sup>, Nattakarn Kruatong <sup>2</sup>, Soydoa Vinitnantharat <sup>2,3,\*</sup>, Ponwarin Wilamas <sup>4</sup>, Rattikan Neamchan <sup>3</sup>, Nareerat Sukkhee <sup>3</sup>, David Werner <sup>5</sup> and Saichol Sanghaisuk <sup>6</sup>

- <sup>1</sup> Chemistry for Green Society and Healthy Living Research Unit (ChGSH), Department of Chemistry, Faculty of Science, King Mongkut's University of Technology Thonburi, Bangkok 10140, Thailand
- <sup>2</sup> Environmental Technology Program, School of Energy, Environment and Materials, King Mongkut's University of Technology Thonburi, Bangkok 10140, Thailand
- <sup>3</sup> Environmental and Energy Management for Community and Circular Economy (EEC&C) Research Group, King Mongkut's University of Technology Thonburi, Bangkok 10140, Thailand
- <sup>4</sup> Department of Biological Science, Faculty of Science, Ubon Ratchathani University, Ubon Ratchathani 34190, Thailand
- <sup>5</sup> School of Engineering, Newcastle University, Newcastle upon Tyne NE1 7RU, UK
- <sup>6</sup> Department of Pollution Control, Ministry of Natural Resources and Environment, Bangkok 10400, Thailand
- \* Correspondence: soydoa.vin@mail.kmutt.ac.th

**Abstract:** Currently, heavy metal-contaminated groundwater is an environmental concern. This study investigated the use of bamboo biochar, chitosan-impregnated biochar, and iron-impregnated biochar for arsenic, iron, and manganese removal from groundwater. Isotherms of arsenic, iron, and manganese adsorption by bamboo derived biochar were compared with those of commercial activated carbon in simulated groundwater composed of single and ternary heavy metal solutions. The binding of heavy metals by virgin and loaded bamboo biochar and activated carbon was also investigated by sequential extraction. Chitosan and iron-impregnated biochar had enhanced arsenic adsorption, but these sorbents turned the pH of solution acidic, while it was alkaline for activated carbon. Adsorption equilibrium times of arsenic and iron were faster for single than ternary heavy metal systems because less ion competition occurred at active sites. The Langmuir model fitted the adsorption data well. The maximum adsorption capacities of arsenic, iron, and manganese by bamboo biochar in ternary heavy metal system were 2.2568, 0.6393, and 1.3541 mg g<sup>-1</sup>, respectively. The main mechanism for arsenic removal was precipitation with iron. Bamboo biochar bound iron in organic and sulfide fractions and manganese with iron-oxide. Bamboo biochar can replace activated carbon as a more efficient and sustainable carbonaceous sorbent material for removal of mixed heavy metals from groundwater within acceptable pH ranges.

**Keywords:** adsorption; fractionation; heavy metal removal; isotherm; modified biochar



**Citation:** Pinisakul, A.; Kruatong, N.; Vinitnantharat, S.; Wilamas, P.; Neamchan, R.; Sukkhee, N.; Werner, D.; Sanghaisuk, S. Arsenic, Iron, and Manganese Adsorption in Single and Ternary Heavy Metal Solution Systems by Bamboo-Derived Biochars. *C* **2023**, *9*, 40. <https://doi.org/10.3390/c9020040>

Academic Editor:  
Dimitrios Kalderis

Received: 28 January 2023  
Revised: 1 April 2023  
Accepted: 12 April 2023  
Published: 16 April 2023



**Copyright:** © 2023 by the authors. Licensee MDPI, Basel, Switzerland. This article is an open access article distributed under the terms and conditions of the Creative Commons Attribution (CC BY) license (<https://creativecommons.org/licenses/by/4.0/>).

## 1. Introduction

Iron (Fe) and manganese (Mn) are ubiquitous in soil and normally found in surface and groundwater from rock weathering. In some regions of Asian countries, heavy metal contamination in water resources was associated with mining, manufacturing, and rock weathering [1,2]. Arsenic (As) is one of the heavy metals causing concern, and about 180 million people are at risk of arsenic poisoning [2]. In addition, environmental impacts will differ between single-metal and mixed-metal pollution [1]. Excessive arsenic, iron, and manganese concentrations were found in groundwater in the rural areas of developing countries where groundwater is the main water resource for drinking water. Groundwater reportedly contained As, Fe, and Mn at maximum concentrations of 0.09, 3.68, and 0.38 mg/L in Jashor, Bangladesh [3]; 0.112, 46.3, and 6.16 mg L<sup>-1</sup> in Shuangliao, China [4]; and 0.416, 68, and 1.9 mg L<sup>-1</sup> in Lampang, Thailand [5]. Iron and manganese are necessary

for human health as iron relates to a wide variety of metabolic processes, including oxygen transport, deoxyribonucleic acid synthesis, and electron transport [6]. Manganese is also essential for development, metabolism, and the antioxidant system [7] serving as a cofactor of several critical enzymes [8]. However, prolonged consumption of high amounts of these heavy metals results in severe health impacts such as organ dysfunction including cell death, fibrosis, and carcinogenesis from iron toxicity [9]; psychiatric symptoms including emotional liability, mania, compulsive or aggressive behavior, irritability, reduced response speed from manganese toxicity [10]; and disturbance in the nervous system, while carcinogenic effects on numerous organs such as lung, urinary tract, and skin result from arsenic toxicity [11]. The maximum concentrations of As, Fe, and Mn for drinking water recommended by the WHO (2017) [12] are 0.01, 0.3, and 0.4 mg L<sup>-1</sup>, respectively. As the excessive presence of As and Mn in water resources is a serious concern to public health, they should be removed to the allowable concentrations by water treatment.

The adsorption process is widely used in water treatment due to its ease of operation and cost-effectiveness. Adsorption is a mass transfer process in which the pollutant from the liquid phase transfer to the solid phase or adsorbent. The porous structure, surface area, and functional groups of adsorbents play an important role in heavy metal removal. Heavy metals tend to adsorb onto the oppositely charged adsorbents. Among the numerous studied adsorbents, biochar has proven to be effective for the removal of heavy metals from water and wastewater due to its negative charge from oxygen functional groups and also other related mechanisms such as complexation, physical sorption, reduction of metal species, electrostatic interactions, and precipitation [13,14]. Thus, biochar is increasingly considered as alternative that can replace commercial activated carbon. Biochar can also be modified on its surfaces with chemicals to improve its adsorption properties. Chitosan impregnation of biochar was reported for the removal of inorganic and organic pollutants including heavy metals [15]. Chitosan is widely used because it is a biodegradable and renewable polymer that possesses both cationic charges (from amino groups-NH<sub>2</sub>) and anionic charges (from hydroxyl groups-OH). Loc et al. [16] reported the removal of an organic dye by chitosan-modified biochar through electrostatic interaction and complexation. Another simple modification of biochar surfaces is iron impregnation for the removal of acid red dye [17], phosphate [18], and arsenic [19,20]. Sun et al. [21] concluded that the main mechanisms for arsenic removal by modified biochars were electrostatic interaction, complexation, and precipitation.

Biochar composition is highly heterogeneous, containing not only the main elements of carbonaceous adsorbents (carbon, hydrogen, and oxygen) but also nutrients (nitrogen, phosphorus, and potassium) and some heavy metals. It was reported that biochar produced from coconut residues and rice straw contains Fe, Zn, and Al [22]. Wang et al. [23] researched the amounts of heavy metals in chicken manure biochar and water-washed swine manure biochar indicating high concentrations of arsenic, chromium, and manganese; however, the proportions of labile fractions were decreased with increased pyrolysis temperature during thermal conversion of biomass. Thus, if biochar is used as adsorbent for water treatment it may release nutrients and heavy metals. It was reported that the release of ions from biochar into deionized water followed the order of Cl<sup>-</sup> > K<sup>+</sup> > Na<sup>+</sup> > PO<sub>4</sub><sup>3-</sup> > SO<sub>4</sub><sup>2-</sup> > Ca<sup>2+</sup> > NO<sub>3</sub><sup>-</sup> > Mg<sup>2+</sup> > NH<sub>4</sub><sup>+</sup> = NO<sub>2</sub><sup>-</sup> and chitosan-impregnated biochar released less ions than unmodified biochar [24]. Previous research mostly evaluated the removal of heavy metals by biochar and modified biochar in single solute systems. Few studies have addressed the removal of mixed heavy metals and considered the fraction of heavy metals in biochar.

Bamboo is abundantly available in tropical and subtropical countries. To increase its stability in the environment, it is necessary to convert raw biomass to biochar. Bamboo may be a promising adsorbent as bamboo biomass has been previously transformed into biochar, activated carbon, and aerogel [25]. Previous research reported the main structural components of bamboo biomass were cellulose and hemicellulose of 47.5 and 15.3%, respectively [26]. A review on bamboo-based biochar indicated the high surface

area and mesoporous structure of bamboo biochar enables it to adsorb antibiotics (fluoroquinolone, sulfamethoxazole, and sulphapyridine), nutrients (ammonium ion, nitrate ion, and phosphate ion), heavy metals (Cd, Cr, and U), dyes (Congo red and acid black 172), and 2,4-dichlorophenol [25]. Hernandez-Mena et al. [26] reported bamboo biochar could adsorb heavy metals with strong adsorption intensity, but less is known about the removal of mixed heavy metals, such as As, Fe, and Mn in a trinary system [26]. In addition, the effects of surface modification on adsorption capacities for a trinary system has also hardly been investigated. Thus, the present study aimed to (i) study the performance of bamboo biochar without and with modification by iron and chitosan impregnation, in comparison with commercial activated carbon, in terms of the adsorption of As, Fe, and Mn in single and trinary systems and (ii) to investigate the labile and stable fractions of heavy metals bound onto bamboo-derived biochars.

## 2. Materials and Methods

### 2.1. Simulated Water Solution

Tap water was used to provide background ions for all experiments. It was analyzed for cations and anions by Ion Chromatography (IC, 761 Compact IC, Metrohm, Switzerland) as shown in Table 1. Before being used, tap water was spiked to achieve the desired concentration of each heavy metal in the preparation of the single or trinary heavy metal solution systems. The Fe(II), Mn(II), and As(V) ions were prepared from  $\text{FeSO}_4 \cdot 7\text{H}_2\text{O}$  (Ajax Finechem Pty Ltd., Taren Point, Australia),  $\text{MnSO}_4 \cdot \text{H}_2\text{O}$  (Ajax Finechem Pty Ltd., Taren Point, Australia), and  $\text{Na}_2\text{HAsO}_4 \cdot 7\text{H}_2\text{O}$  (Sigma-Aldrich, St. Louis, MO, USA) salts in analytical grade, respectively.

**Table 1.** Background ions in simulated groundwater solution.

Ions	$\text{Na}^+$	$\text{NH}_4^+$	$\text{K}^+$	$\text{Ca}^{2+}$	$\text{Mg}^{2+}$	$\text{Cl}^-$	$\text{NO}_3^-$	$\text{SO}_4^{2-}$	$\text{PO}_4^{3-}$
( $\text{mg L}^{-1}$ )	11.95	0.03	4.66	57.05	9.52	12.75	4.03	34.89	ND

Note: ND = not detectable.

### 2.2. Bamboo-Derived Biochars and Characterization

Bamboo biochar (B) was derived from Ubon Ratchathani province, Thailand. Bamboo stem (*Bambusa beecheyana*) at the age of 2–3 years were cut into lengths of 30 cm and then the cuttings were placed in a traditional earth mound kiln (hemispherical shape with diameter of 2.5 m and height of 2.5 m). Carbonization was completed within 6 days with the temperatures range 400–600 °C. Then, the kiln was left to cool for 6 days, and biochar was taken out from the kiln. It was crushed to a uniform size in the range of 2.0–3.0 mm. All experiments used same batch of biochar production.

Chitosan-impregnated bamboo biochar (BC) was prepared following Vinitnantharat et al. [27] by placing 5 g crushed B in 100 mL chitosan solution in a 250 mL Erlenmeyer flask. Then, the suspension was agitated in a shaker at 100 rpm for 24 h at room temperature (30 °C). The chitosan solution was prepared by dissolving 1 g chitosan powder in 100 mL of 1% ( $v v^{-1}$ ) acetic acid. BC was separated from the mixture and rinsed with tap water until the pH of the wash water reached  $7.0 \pm 0.5$ . BC was rinsed with deionized water (200 mL) and air dried for 2 days before storage in a bottle.

Iron-impregnated bamboo biochar (BFe) was prepared by adapting the method of Kalaruban et al. [28]. A total of 20 g of crushed B was mixed with 1.35 % ( $w v^{-1}$ ) of  $\text{FeCl}_3 \cdot 6\text{H}_2\text{O}$  solution in a 250 mL Erlenmeyer flask. Then, the suspension was agitated in a shaker at 100 rpm for 24 h at room temperature (30 °C). BFe was separated from the mixture by filtering through a plastic sieve, then it was rinsed with tap water until pH was  $7.0 \pm 0.5$  and rinsed with deionized water (200 mL). BFe was left to dry at room temperature and then kept in a bottle.

Commercial activated carbon (AC) in the size of 2.0–3.0 mm was obtained from Charcoal Home Co., Ltd., Bangkok, Thailand. It was made from bamboo (*Dendrocalamus asper*) by carbonization in a brick kiln at high temperature (1000 °C). It was used as received.

Adsorbents were characterized by the physical adsorption of nitrogen gas according to the method of Brunauer, Emmet, and Teller (BET, Quantachrome, Quandrasorb evo, Anton Paar GmbH, Graz, Austria); the surface features and morphology were studied by a Scanning Electron Microscope and Energy Dispersive X-ray Spectrometer (SEM-EDS, Jeol, JSM-7610F Plus, Japan); surface functional groups were characterized by Fourier transform infrared spectroscopy (FTIR, Thermo Scientific Nicolet 6700, Waltham, MA, USA); and chemical composition was studied by X-ray fluorescence (XRF, Rigaku, ZSX Primus II, Japan).

Iodine number was analyzed to determine the iodine adsorption following the ASTM D4607 method. The pH of each biochar was measured after shaking 5 g of biochar in 50 mL of deionized water (pH<sub>DI</sub>) at 100 rpm at 30 °C and the pH at point of zero charge (pH<sub>pzc</sub>) was analyzed following the method of Khawkomol et al. [22]. The pH value was measured by a pH meter (pH3210, WTW, Weilheim, Germany).

### 2.3. Adsorption Equilibration Time Study

The adsorption equilibration time was performed for single and ternary heavy metal solution systems. The single heavy metal system was performed using 0.5 g of adsorbents with 50 mL of solution containing 0.05 mg L<sup>-1</sup> As(V), or 7.0 mg L<sup>-1</sup> Fe(II), or 1.0 mg L<sup>-1</sup> Mn(II) in 100 mL plastic bottles. As for ternary heavy metal system, the concentrations of As(V), Fe(II), and Mn(II) were 0.02, 7.0, and 1.0 mg L<sup>-1</sup>, respectively. The solution pH was adjusted to 7.00 ± 0.50, except that it was 4.40 ± 0.50 for adsorption of single Fe(II) solution to avoid iron precipitation. The mixtures were agitated in an incubator shaker at 100 rpm and temperature of 28 ± 0.5 °C. After contact time at 2, 5, 12, 24, 36, 48, 72, 84, 96, 108, 120, 132, 144, and 156 h, the mixture was passed through a 0.45 µm nylon membrane and the filtrate was analyzed for As(V) using an inductively coupled plasma-optical emission spectrometer (ICP-OES, Perkin Elmer Optima 8000), and for Fe(II) and Mn(II) using an atomic absorption spectrometer (AAS, Shimadzu Europa AA-6300, Japan). All experiments were performed in duplicate. The amount of Fe, Mn, and As adsorbed onto the adsorbent,  $q$  (mg g<sup>-1</sup>), was calculated using Equation (1):

$$q_t = [(C_0 - (C_t - C_c)) \cdot V] / m \quad (1)$$

where  $C_0$  is the initial concentration of heavy metal ion (mg L<sup>-1</sup>),  $C_t$  is the concentration of heavy metal ions at time  $t$  (mg L<sup>-1</sup>),  $C_c$  is the concentration of heavy metal ions released by adsorbent into simulated water solution for the same condition of heavy metal ions adsorption at time  $t$  (mg L<sup>-1</sup>),  $V$  is the volume of solution (L), and  $m$  is the mass of adsorbent (g).

### 2.4. Isotherm Study

The batch adsorption experiments consisted of single and tri-heavy metals solutions for determining the adsorption capacities of each biochar type. Adsorption studies were performed in 100 mL bottles shaken in an incubator shaker at 100 rpm and temperature of 28 ± 0.5 °C until reaching equilibrium.

For single heavy metal isotherm experiments, a biochar dosage of 0.5 g was contacted with 50 mL simulate water solution containing different concentration of As(V) 0.01–0.10 mg L<sup>-1</sup> or Fe(II) 1.00–10.00 mg L<sup>-1</sup> or Mn(II) 1.00–18.00 mg L<sup>-1</sup>. The pH of the solution was adjusted to 7.00 ± 0.50, except it was 4.40 ± 0.50 for Fe(II) adsorption. In the case of the ternary heavy metal system, different masses of biochars (0.2–1.0 g) were contacted with fixed concentrations of 0.02 mg L<sup>-1</sup> As(V), 7.0 mg L<sup>-1</sup> Fe(II), and 1.0 mg L<sup>-1</sup> Mn(II) in 50 mL simulated water solution. The initial and final equilibrium concentrations were measured for each heavy metal and used for the construction of isotherm curves. The pH of the solution at equilibrium (pH<sub>E</sub>) was also measured.

Two adsorption models, Freundlich and Langmuir, were used to fit the experimental data. The Freundlich model is an empirical model suitable for nonideal adsorption on heterogeneous surfaces as expressed in Equation (2).

$$q_e = K_F C_e^{1/n}, (0 < 1/n < 1) \quad (2)$$

where  $q_e$  is the amount of heavy metal adsorbed at equilibrium ( $\text{mg g}^{-1}$ ),  $C_e$  is the heavy metal concentration at equilibrium ( $\text{mg L}^{-1}$ ),  $K_F$  is the Freundlich constant related to maximum adsorption capacity ( $(\text{mg g}^{-1})(\text{L mg}^{-1})^{1/n}$ ), and  $1/n$  is the Freundlich constant relate to the intensity (dimensionless).

The Langmuir adsorption model has been used to describe the uniform energies of adsorption onto the surface and no transmigration of adsorbate in the plane of the surface. The Langmuir model is given by Equation (3).

$$\frac{C_e}{q_e} = \frac{1}{K_L q_m} + \frac{C_e}{q_m} \quad (3)$$

$q_m$  defines the maximum amount of heavy metal per unit weight of adsorbent to form a complete monolayer coverage on the surface ( $\text{mg g}^{-1}$ ), and  $K_L$  is the Langmuir constant ( $\text{L mg}^{-1}$ ).

### 2.5. Fractionation Analysis

The distribution pattern of heavy metals bound on the specific functional groups of selected biochars was investigated by using biochar before and after being loaded with trinary heavy metal solution (biochar dosage  $1\% w v^{-1}$ ). Two grams of biochar were sequential extracted into 6 fractions: F1 Water soluble (Soluble); F2 Exchangeable (Exch); F3 Bound to carbonate ( $\text{CO}_3$ ); F4 Bound to Fe/Mn oxides (Fe/MnO); F5 Bound to organic matter and sulfide (Org/S); and F6 Residual. The extraction method was adapted from Kashem et al. [29] as shown in Table 2. All extracts were centrifuged for 10 min at 3000 rpm to separate the residue and supernatant. The supernatant was filtered and adjusted to  $\text{pH} < 2$  for analysis of As(V), Fe(II), and Mn(II).

**Table 2.** Sequential extraction procedures.

Fraction	Extractants	Extraction Conditions
F1 Soluble	20 mL of deionized water	Shaking at room temperature for 1 h
F2 Exch	20 mL of 1 M $\text{NH}_4\text{OAc}$ , pH 7	Shaking at room temperature for 2 h
F3 $\text{CO}_3$	20 mL of 1 M $\text{NH}_4\text{OAc}$ , pH 5	Shaking at room temperature for 2 h
F4 Fe/MnO	20 mL of 0.04 M $\text{NH}_2\text{OH.HCl}$ in 25% acetic acid ( $v v^{-1}$ ), pH 3	Placing in the water bath at $80^\circ\text{C}$ for 6 h
F5 Org/S	15 mL of 30% $\text{H}_2\text{O}_2$ ( $v v^{-1}$ ), after being cooled add 5 mL of 3.2 M $\text{NH}_4\text{OAc}$ in 20% $\text{HNO}_3$ ( $v v^{-1}$ )	Placing in the water bath at $80^\circ\text{C}$ for 5.5 h Shaking at room temperature for 0.5 h
F6 Residual	20 mL of 7 M $\text{HNO}_3$	Placing in the water bath at $80^\circ\text{C}$ for 6 h

The percentage of a heavy metal in each fraction ( $F_i$ ) was calculated following Equation (4)

$$\% \text{Fraction}(i) = \frac{100 \times F_i}{(F1 + F2 + F3 + F4 + F5 + F6)} \quad (4)$$

### 3. Results

#### 3.1. Biochar Characteristics

Table 3 shows the chemical and physical properties of each biochar. Results from XRF revealed that there were Fe and Mn in all bamboo-derived biochars and activated carbon, but arsenic was not detected. The highest content of metal from XRF analysis of B and AC was potassium (K). Chongtham et al. [30] reported that potassium was the main metal in bamboo shoot ranging from 41.90–66.60% whereas Fe and Mn were in the range from 0.047–0.10% and 0.012–0.097%, respectively. The oxides of calcium (Ca) and K could be hydrated to  $\text{Ca}(\text{OH})_2$  and KOH, respectively, and produce alkaline solutions. The  $\text{pH}_{\text{DI}}$  of AC was higher than B because it contains more base cations. Impregnation of chitosan and iron changed the elemental composition and decreased  $\text{pH}_{\text{DI}}$ . BC was prepared by coating chitosan on B, for which chitosan was dissolved in acetic acid solution. Thus, metals in B were released particularly for easily soluble metal such as potassium, resulting in higher relative contents of other metal contents than B. In addition, the percentages of Fe, Ca, silica (Si), magnesium (Mg), and phosphorus (P) were increased. Fe and chloride (Cl) contents were high in BFe because of the impregnation by  $\text{FeCl}_3$ . The  $\text{pH}_{\text{DI}}$  of BFe was lowest compared to the other adsorbents as the hydrolysis of  $\text{Fe}^{3+}$  formed  $\text{FeOH}^{2+}$  and released hydrogen ions ( $\text{H}^+$ ). BC and BFe had  $\text{pH}_{\text{DI}}$  lower than  $\text{pH}_{\text{pzc}}$ , hence their surfaces exhibited a net positive charge. BET surface area ( $S_{\text{BET}}$ ) and pore volume ( $V_p$ ) of BC and BFe were lower than B indicating that impregnation was achieved. However, pore diameters ( $D_p$ ) of BC and BFe were closed to the original biochar (B). Iodine number measures the elementary iodine ( $\text{I}_2$ ) which has a statistical radius of 2.46 Å [31]. Ferric chloride was used for impregnation and the  $\text{Fe}^{3+}$  with a radius of 0.65 Å [32] could fill up the micropores. The  $D_p$  of AC was less than B according to the pyrolysis temperature of AC was 1000 °C higher than those of B. Sahool et al. [33] reported the evolution of micropores in the biochar leads to a decrease in pore diameter at high pyrolysis temperature. This result agrees with the remarkably high iodine number of AC indicating its microporous structure.

**Table 3.** Chemical and physical characteristics of bamboo-derived biochar.

	Metal Composition (%)										$S_{\text{BET}}$ ( $\text{m}^2$ $\text{g}^{-1}$ )	$V_p$ ( $\text{cm}^3$ $\text{g}^{-1}$ )	$D_p$ (Å)	$\text{pH}_{\text{DI}}$	$\text{pH}_{\text{pzc}}$	Iodine Number ( $\text{mg g}^{-1}$ )
	Mn	Fe	Ca	Si	S	P	Cl	Mg	As	K						
B	0.70	0.32	7.78	7.93	2.87	7.06	5.62	2.69	ND	64.5	191.9	0.10	21.64	8.66	7.63	75.30
BC	1.68	0.82	13.7	14.5	6.44	10.9	ND	3.41	ND	47.7	66.6	0.04	21.96	4.31	4.56	72.09
BFe	0.59	19.6	3.17	25.9	3.08	6.04	24.3	1.39	ND	13.2	127.7	0.07	22.06	2.59	3.61	45.54
AC	0.88	2.21	9.77	9.62	1.04	2.41	4.44	3.60	ND	65.7	136.0	0.11	19.52	9.35	8.34	267.38

The SEM images of biochar samples confirmed the high porosity of biochar with longitudinal pores originating from the vascular bundles of bamboo, whereas AC showed cracked surfaces (Figure 1). Chitosan was mostly impregnated on the surfaces, whereas iron was impregnated in the mesopores and micropores of biochar. AC had irregular surfaces and porous structure. In addition, there were some particles on the surfaces. Result from EDS revealed that carbon (C) content was high in B, BC, and AC, ranging from 76.24 to 88.51%, followed by oxygen (O), ranging from 7.84 to 25.37%. After chitosan impregnation of biochar, the lower percentage of carbon content and higher oxygen content suggested the presence of chitosan on the BC surface. As for BFe, the C and O contents were 33.46% and 25.37%, respectively. The O/C ratio of BFe was highest at 0.76, followed by BC, B, and AC, at 0.16, 0.08, and 0.09, respectively, indicating the increased oxygen functional groups on BFe surfaces. The low O/C ratio of B and AC was due to the loss in oxygen functional groups such as hydroxy, carboxyl, and carbonyl groups in the thermo-conversion process. At pyrolysis temperature of 300–400 °C, cellulose and hemicellulose are decomposed and lignin is decomposed above 400 °C [34]. However, Mn was found at the outer surfaces of

BC and BFe at 6.08% and 2.39%, respectively. This is due to the acid solution of BC and BFe which enhanced Mn mobility allowing its transport from the inner layers to outer surfaces. The stability of biochar can be estimated from the O/C ratio and the O/C of BFe was greater than 0.6, indicating a half-life of less than 100 years whereas the O/C of the rest of the biochars were less than 0.2 implying a half-life of more than 1000 years [35].

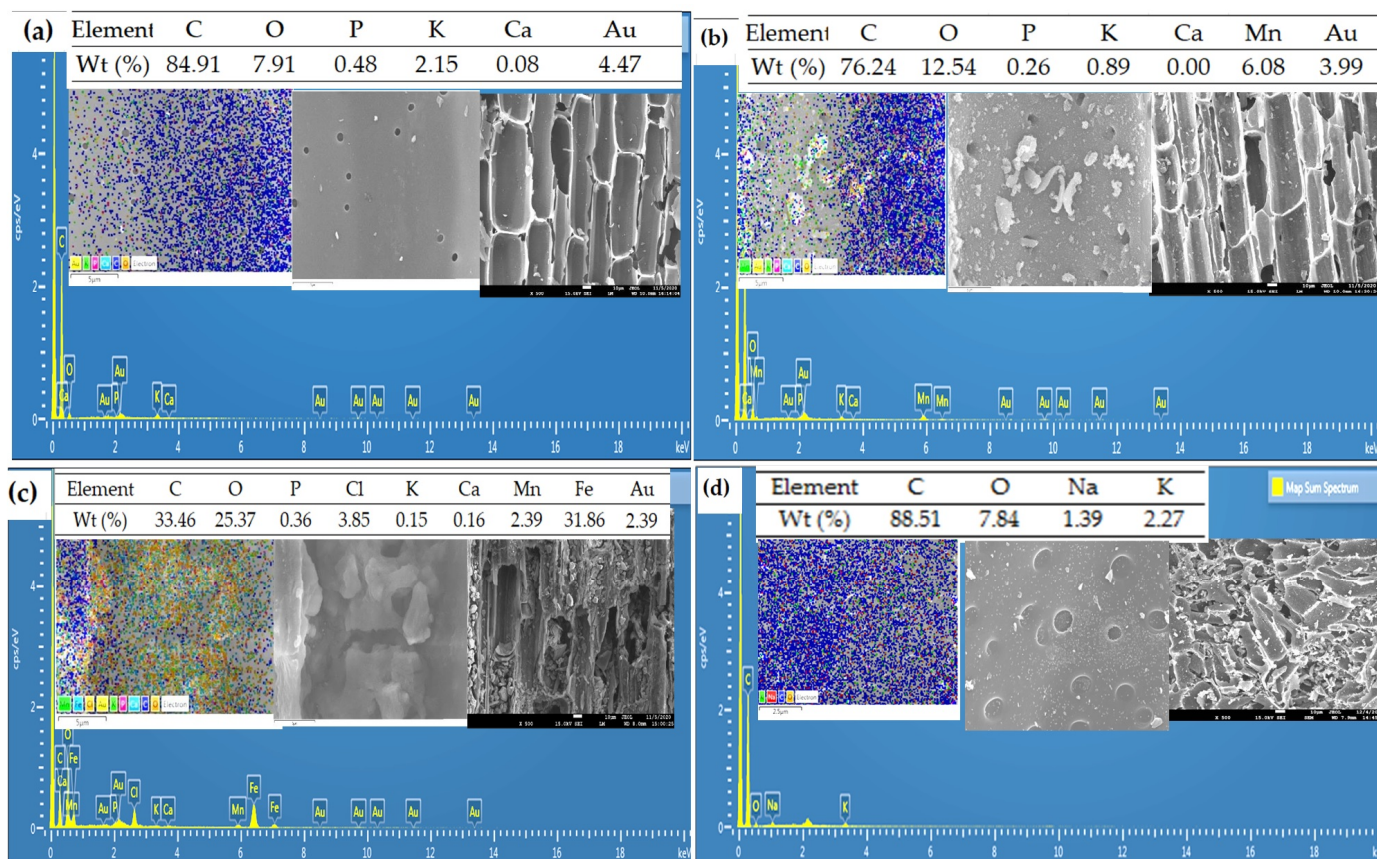


**Figure 1.** SEM-EDS images of bamboo-derived biochars. (a) B (b) BC (c) BFe (d) AC.

### 3.2. Adsorption Equilibration Time

Adsorption equilibration times of As and Fe in the single heavy metal system were faster than in the ternary system because heavy metal ions in the ternary system competed for the same active sites of biochar. BC and BFe reached equilibrium for As adsorption in the single heavy metal system at 5 and 2 h, respectively, which was faster than B and AC that reached equilibrium at 12 h (Figure 2a). Dissolved As(V) is negatively charged at neutral pH so it reacted with the positively charged surfaces of BC and BFe. Likewise, Fe (II) adsorption also reached equilibrium within 3 h for B and AC because of the opposite charge of adsorbent and adsorbate (Figure 2b). It took 12 and 48 h for BC and BFe, respectively, to reach Fe adsorption equilibrium in the single heavy metal system. Adsorption of Mn(II) required more time than As and Fe adsorption in the range of 72–108 h. In addition, the equilibration times of Mn adsorption in the single system were the same as in the ternary system (Figure 2c).

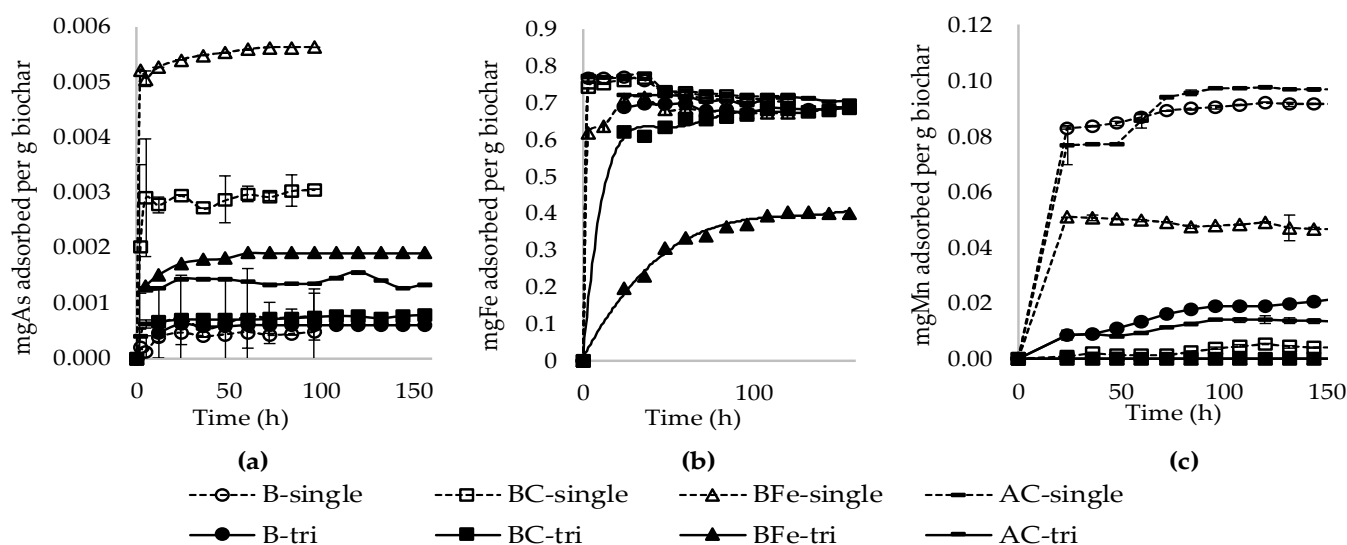


**Figure 2.** Equilibration time of (a) As(V), (b) Fe(II), and (c) Mn(II) adsorption in single and trinary heavy metal systems by different biochars and activated carbon.

### 3.3. Single Heavy Metal Solution Adsorption

Freundlich and Langmuir adsorption isotherms are widely used to explain the adsorption on heterogeneous and homogeneous of adsorbent surfaces, respectively. The corresponding parameters, correlation coefficients ( $R^2$ ), and  $pH_E$  are listed in Table 4. The  $R^2$  values calculated for each model indicated that the adsorption data by B and BC were more suitable described by the Langmuir model than by the Freundlich model. The Langmuir model also provided the best fit for Mn adsorption by BFe, and for As and Fe adsorption by AC. In addition, kinetic studies from previous work also revealed that the adsorption of As(V), Fe(II), and Mn(II) by all adsorbents were following pseudo-second order kinetics. This indicates that adsorption could be achieved via chemical processes [36]. The  $q_m$  from the Langmuir model revealed that chitosan impregnation enhanced all heavy metals adsorption, whereas iron impregnation enhanced only As adsorption. The highest As adsorption was  $0.019 \text{ mg g}^{-1}$  by BFe, and the highest Fe and Mn adsorption were  $303.03$  and  $5.2029 \text{ mg g}^{-1}$  by BC. BFe and BC significantly removed As and Fe, respectively. It shows that  $q_m$  values of BFe to remove As were higher than  $q_m$  values of B, BC and AC of 3.36, 2.03 and 10.83 times, respectively. The  $q_m$  values of BC were higher than  $q_m$  values of B, BFe, and AC of 1.76, 7.12, and 22.70 times for removal of Fe, respectively. Other work on iron-modified biochar reported high  $q_m$  for As(V) adsorption of  $0.926 \text{ mg g}^{-1}$  by palm leave biochar [37] and  $0.19 \text{ mg g}^{-1}$  by parsley leaf biochar [38]; however, those As(V) concentrations were higher in the ranges of  $0.5\text{--}30 \text{ mg L}^{-1}$  and  $0.05\text{--}2.00 \text{ mg g}^{-1}$ , respectively, compared to the present study of  $0.01\text{--}0.1 \text{ mg L}^{-1}$ .

**Table 4.** Isotherm parameters and correlation coefficients for As, Fe, and Mn adsorption in the single heavy metal system.

Adsorbent	Heavy Metal	Freundlich			Langmuir			pH <sub>E</sub>
		K <sub>F</sub> (mg g <sup>-1</sup> ) (L mg <sup>-1</sup> ) <sup>1/n</sup>	1/n	R <sup>2</sup>	q <sub>m</sub> (mg g <sup>-1</sup> )	K <sub>L</sub> (L mg <sup>-1</sup> )	R <sup>2</sup>	
B	As (V)	0.0044	0.8435	0.9215	0.0058	0.7986	0.9630	7.98–8.78
	Fe(II)	353.25	0.9353	0.9450	172.41	0.3621	0.9482	8.00–8.33
	Mn (II)	1.1410	0.7727	0.9911	5.0226	3.3451	0.9914	8.19–8.59
BC	As (V)	0.0594	0.7384	0.8924	0.0096	0.0334	0.9162	5.00–5.33
	Fe(II)	274.21	0.9513	0.9959	303.03	0.9091	0.9966	6.13–6.34
	Mn (II)	0.0260	1.0336	0.9230	5.2029	181.92	0.9914	4.96–5.94
BFe	As (V)	0.1018	0.5052	0.9050	0.0195	0.0087	0.8639	6.05–6.98
	Fe(II)	97.55	0.8309	0.7684	42.55	0.2128	0.8971	6.33–6.37
	Mn (II)	0.0515	0.7436	0.9449	0.2170	2.6296	0.8137	5.03–6.96
AC	As (V)	0.0038	0.6713	0.8499	0.0018	0.1268	0.8889	9.32–9.50
	Fe(II)	25.23	0.2672	0.8541	13.35	0.0080	0.8153	8.95–8.99
	Mn (II)	2.5796	0.3375	0.9222	4.8355	0.4265	0.9317	8.89–9.24

BC gave high adsorption capacities because chitosan has free amino and hydroxyl groups for interaction with negative and positive charges of heavy metals, respectively. The pK<sub>a</sub> of the amino group in chitosan ranges from 6.2–7.0 [39]. Hence, at a solution pH below 6.2 the amino group is protonated. Reportedly, the extent of protonation is 9, 50, 91, and 99 % at pH 7.3, 6.3, 5.3, and 4.3, respectively [40]. The pH of solution also affects the adsorbent surfaces and the specification of heavy metals. The speciation of As at different pHs is shown in Equations (5)–(7) [41].



The adsorption experiments for As adsorption were performed at the initial pH of 7.00 ± 0.50. Use of BC as adsorbent could decrease the pH values and the pH<sub>E</sub> for As adsorption were in the range of 5.00–5.33. Thus, the main speciation of As was H<sub>2</sub>AsO<sub>4</sub><sup>-</sup>, whilst the amino and hydroxyl groups of BC were protonated. These protonated groups at acidic pH result in electrostatic attractions with negatively charge arsenate species. At the solution pH below pH<sub>pzc</sub>, anions favor to adsorb on the adsorbent surfaces. The pH<sub>pzc</sub> values of B and AC were 7.63 and 8.34, respectively, enabling adsorption of HAsO<sub>4</sub><sup>-</sup> species. As for BFe, the main mechanisms for arsenate removal were the surface complexation with iron oxyhydroxide and partial inclusion into the crystalline iron oxides [20,28].

The initial pH for Fe adsorption is 4.40 ± 0.50, which is lower than pH<sub>pzc</sub> of B, BC, and AC, indicating these adsorbents exhibit positive charge. Thus, the repulsion of Fe<sup>2+</sup> could occur. BFe exhibits negative charge resulting in electrostatic attraction. However, the pH values were increased after contacting with adsorbents. This was due to the release of base cations and hydroxide ions from adsorbents into solution. The pH<sub>E</sub> values of B and AC were alkaline (8.00–8.99), whereas the pH<sub>E</sub> values of BC and BFe ranged from 6.13–6.37. In the agitation during adsorption experiments, Fe<sup>2+</sup> could be oxidized to Fe(OH)<sub>3</sub>. Hove et al. [41] expressed that the oxidation rate at pH 9.0 was higher than at pH 6.0. The results agree with the study of contact time showing B and AC reached equilibration times faster than BC and BFe.

Adsorption of Mn was performed at neutral pH; thus, the main species was  $Mn^{2+}$ . The  $pH_{pzc}$  values of all adsorbents were lower than  $pH_E$  indicating favorable conditions to adsorb  $Mn^{2+}$ . The formation of manganese oxide ( $MnO_2$ ) from aeration at pH below 9.0 is a slow process and may not be achieved [42]. Because of this, Mn is hardly removed via adsorption.

It should be noted that  $R^2$  values of the Freundlich model were closed to those of the Langmuir model, therefore, heavy metals possibly adsorbed in the inner pores. The radius of  $H_2AsO_4^-$ ,  $Fe^{2+}$  and  $Mn^{2+}$  are 2.27, 0.77, and 0.83 Å [32], respectively which are smaller than pore diameters of the adsorbents. In addition, multilayer adsorption such as surface complexation may have occurred as the simulated groundwater contains cations and anions.

The  $pH_E$  values of BC were lower than 6.0 for As and Mn adsorption which was outside the allowable range of pH 6.5–9.2 of drinking water standards in Thailand [43]. Thus, it may not be suitable for groundwater treatment as low pH could corrode and induce the release of other ions from the adsorbent. Hence, B, BFe, and AC were selected for the trinary adsorption experiments.

### 3.4. Trinary Heavy Metal Solution Adsorption

Arsenic was completely removed from the trinary heavy metal system by adsorption; therefore, the data could not be fitted by the adsorption models. Saikia et al. [44] also reported that iron oxide coated sand and other adsorbents removed As(III) 100 % from water at concentration ranges 0.6–1.0  $mg L^{-1}$  in the presence of Fe(II) and Mn(II). The initial pH of solution was  $7.00 \pm 0.50$ . After being agitated,  $Fe^{2+}$  was oxidized to  $Fe^{3+}$  and then it could react with As(V) to ferric arsenate (i.e.,  $FeAsO_4$ ). Table 5 shows that the Langmuir model provides the best fit for Fe and Mn adsorption by B and BFe, and for Fe adsorption by AC.

**Table 5.** Isotherm parameters and correlation coefficients for Fe and Mn adsorption in trinary system.

Adsorbent	Heavy	Freundlich			Langmuir		$pH_E$	
	Metal	$K_F$ ( $mg g^{-1}$ ) ( $L mg^{-1}$ ) <sup>1/n</sup> )	1/n ( $L g^{-1}$ )	$R^2$	$q_m$ ( $mg/g^{-1}$ )	$K_L$ ( $L mg^{-1}$ )		$R^2$
B	Fe(II)	2.6710	0.6808	0.8022	2.2568	0.3056	0.8360	6.82–8.44
	Mn(II)	0.2559	0.6979	0.9020	0.6393	1.5398	0.9155	
Bfe	Fe(II)	36.874	0.7530	0.8686	26.1780	0.3010	0.9008	5.58–6.80
	Mn(II)	0.2715	0.8946	0.8388	3.6643	12.342	0.8732	
AC	Fe(II)	3.6370	0.8387	0.8632	3.1756	0.5062	0.8868	6.80–9.47
	Mn(II)	0.2142	0.8680	0.9031	1.3541	5.3369	0.8823	

The  $q_m$  values show that adsorption of Fe and Mn is in the order of BFe > AC > B. The  $q_m$  values from trinary heavy metal adsorption experiments were less than  $q_m$  values from single heavy metal adsorption, except for Mn adsorption by BFe. The  $pH_E$  values of BFe were far higher than  $pH_{pzc}$  (3.61), because of the negative charge of BFe surfaces. AC had higher adsorption than B because its porous structure enabled adsorption of heavy metals in the inner pores. In addition, Mn can be oxidized to  $MnO_2$  at pH 9. To examine the main functional groups for heavy metal adsorption, the FTIR spectra of virgin and loaded B, BFe, and AC were compared in Figure 3.

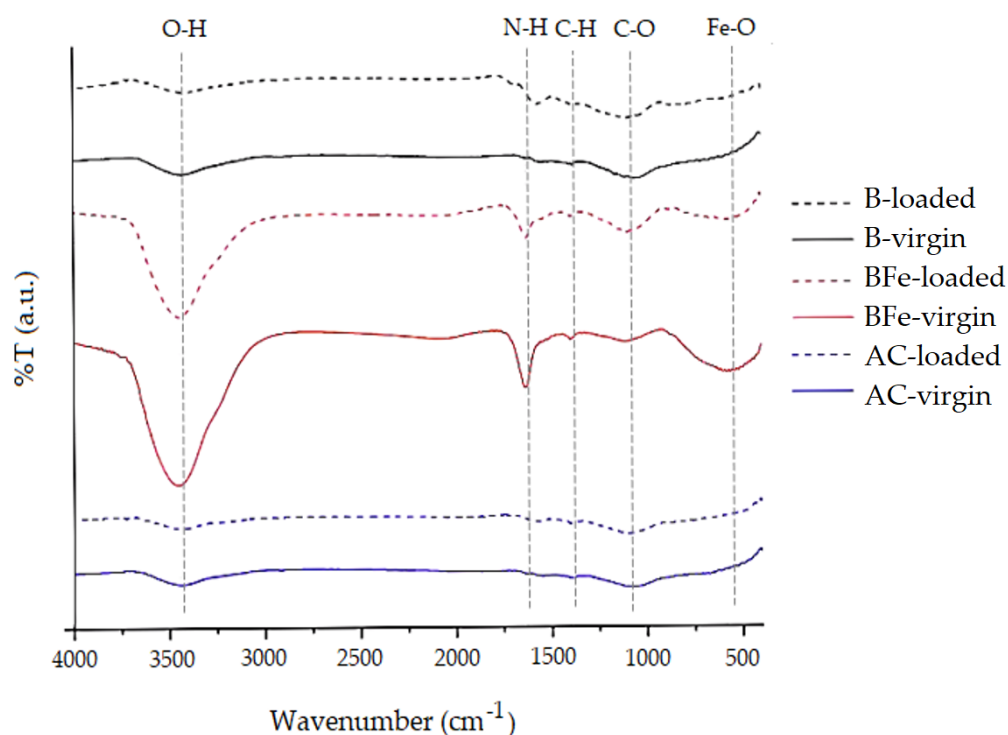


**Figure 3.** Infrared spectra of virgin and loaded B, BFe, and AC.

The spectral bands obtained at 3200–3600  $\text{cm}^{-1}$  were attributed to the O-H stretching vibration of alcohols [45]. The band ranges 1550–1640  $\text{cm}^{-1}$  were denoted as N-H stretching vibration of amides [45], and ranges 1400–1450  $\text{cm}^{-1}$  was the C-H bending vibration of alkanes [45]. The spectral bands at 1000–1300  $\text{cm}^{-1}$  were attributed C-O stretching vibration of ethers. The peaks of virgin adsorbents were similar to the peaks of loaded adsorbents, but the peak intensities of loaded B and AC were smaller than those of virgin B and AC, especially for the O-H group. This indicates the binding of Fe(II) and Mn(II) by this group. Virgin and loaded BFe were found to have additional peaks at 582 and 597  $\text{cm}^{-1}$ , respectively, which represented the Fe-O bond from iron impregnation [46]. The intensity of characteristic bands of AC was low comparing to the bands of B and BFe because the high pyrolysis temperature (1000 °C) for AC preparation could degrade cellulose, hemicellulose, and lignin. The presence of O-H, N-H and C-O functional groups confirms their availability for adsorption via different mechanisms.

### 3.5. Fraction of Heavy Metal Adsorption onto Bamboo Biochar and Activated Carbon

Table 6 presents the distribution pattern of As, Fe, and Mn in virgin and loaded B and AC. As was not found in virgin B, but small amounts were found in F1 and F4 of virgin AC. After loading with mixed heavy metals, As contents were found in F1. Fe was found in all fractions, except in F3 in both virgin B and AC, and was predominantly in F6 for virgin B at 76.2%, and in virgin AC at 47.6%. Fe in the soluble fraction may have reacted with As and precipitated from the solution, thus As was found in the soluble form after being loaded onto the adsorbents. Fe content was decreased after adsorption indicating Fe also reacted with other anionic ions such as sulfate ions. The main fraction of Fe after adsorption was in F5 for B and in F6 for AC. Mn fractions in virgin B and AC were in the following order: F6 > F4 > F5~F2 > F1. It previously reported that the highest Mn fraction was found in the residual fraction (F6) in goat manure biochar and bound to organic matter (F5) in swine manure biochar [47]. Once B and AC were loaded with heavy metals, the metals were mainly found in the fractions F4 and F3. Since F1, F2, and F3 are weakly binding, it was found that Mn is more present in mobile fractions than Fe. The mobile fractions of Mn after being adsorbed were 44.15 and 41.03% for B and AC, respectively.

**Table 6.** Comparison of As, Fe, and Mn contents in each fraction of virgin and loaded B and AC.

Metal	Adsorbents		Fractions (mg kg <sup>-1</sup> )						Total
			F1 Soluble	F2 Exch	F3 CO <sub>3</sub>	F4 Fe/MnO	F5 Org/S	F6 Residual	
As	B	Virgin	0.00 ± 0.00	0.00 ± 0.00	0.00 ± 0.00	0.00 ± 0.00	0.00 ± 0.00	0.00 ± 0.00	0.00 ± 0.00
		Loaded	0.02 ± 0.00	0.00 ± 0.00	0.00 ± 0.00	0.00 ± 0.00	0.00 ± 0.00	0.00 ± 0.00	0.02 ± 0.00
AC	Virgin	0.04 ± 0.00	0.00 ± 0.00	0.00 ± 0.00	0.00 ± 0.00	0.00 ± 0.00	0.00 ± 0.00	0.00 ± 0.00	0.04 ± 0.00
	Loaded	0.01 ± 0.01	0.00 ± 0.00	0.00 ± 0.00	0.00 ± 0.00	0.00 ± 0.00	0.00 ± 0.00	0.00 ± 0.00	0.01 ± 0.01
Fe	B	Virgin	0.23 ± 0.01	1.20 ± 0.42	0.00 ± 0.00	2.03 ± 0.95	9.45 ± 3.45	41.47 ± 3.99	54.40 ± 3.99
		Loaded	0.41 ± 0.19	1.36 ± 0.26	2.44 ± 0.30	9.35 ± 0.13	14.75 ± 2.73	7.98 ± 2.18	36.29 ± 2.73
AC	Virgin	0.20 ± 0.06	0.34 ± 0.16	0.00 ± 0.00	94.64 ± 7.41	9.61 ± 1.65	95.21 ± 18.16	200.01 ± 18.16	
	Loaded	0.41 ± 0.06	0.77 ± 0.00	0.62 ± 0.23	54.46 ± 4.07	3.97 ± 1.44	72.73 ± 12.32	132.96 ± 12.32	
Mn	B	Virgin	0.67 ± 0.02	3.55 ± 0.28	8.32 ± 0.06	11.84 ± 3.79	9.15 ± 0.37	14.00 ± 1.69	47.53 ± 3.79
		Loaded	0.34 ± 0.04	15.83 ± 1.36	22.91 ± 0.88	24.24 ± 0.04	12.57 ± 0.64	12.64 ± 0.24	88.54 ± 1.36
AC	Virgin	0.00 ± 0.00	0.14 ± 0.09	0.72 ± 0.01	2.22 ± 0.20	0.91 ± 0.14	2.98 ± 0.39	6.97 ± 0.39	
	Loaded	0.00 ± 0.00	1.88 ± 0.36	3.82 ± 0.29	4.65 ± 0.48	1.30 ± 0.09	2.26 ± 0.25	13.92 ± 0.36	

#### 4. Discussion

Bamboo biochar can replace commercial activated carbon for heavy metal removal from groundwater. Bamboo biochar and activated carbon had the same functional groups of O-H, N-H, C-H and C-O. The pH of solution and heavy metal speciation influenced the adsorption of As(V), Fe(II), and Mn(II) both in single and ternary heavy metal systems. The pH values of treated water after heavy metal adsorption by bamboo biochar were in the range suitable for drinking water production, whereas AC produced alkaline water, and BC and BFe produced acidic water. However, the maximum adsorption of As(V), Fe(II), and Mn(II) were improved for the chitosan or iron impregnated biochars. BC and BFe can thus be used for removal of As, Fe, and Mn contamination in groundwater, but pH needs readjustment to the acceptable values for drinking water. In addition, treated water should be analyzed for other heavy metals which may be released from biochar. Further work should scrutinize the chemicals used for impregnation and the release of other heavy metals after adsorption. BC and BFe may also be suitable for removal of high concentration of heavy metals such as from mining wastewater.

**Author Contributions:** Conceptualization, S.V.; Funding acquisition, S.V.; Investigation, A.P., N.K., P.W., R.N. and N.S.; Writing—original draft, S.V.; Writing—review and editing, A.P., S.V., D.W. and S.S. All authors have read and agreed to the published version of the manuscript.

**Funding:** This research was funded by the National Research Council of Thailand, grant number NRCT.MHESI(A)(PS)/122/2563.

**Data Availability Statement:** Not applicable.

**Acknowledgments:** Additional supports for biochar characterization were provided by the School of Energy, Environment and Materials and from the study of Kruatong N. through Petchra Pra Jom Klao Ph.D. Research Scholarship (No. 54/2564), King Mongkut's University of Technology Thonburi.

**Conflicts of Interest:** The authors declare no conflict of interest.

#### References

- Zhou, Q.; Yang, N.; Li, Y.; Ren, B.; Ding, X.; Bian, H.; Yao, X. Total Concentrations and Sources of Heavy Metal Pollution in Global River and Lake Water Bodies from 1972 to 2017. *Glob. Ecol. Conserv.* **2020**, *22*, e00925. [[CrossRef](#)]
- Shaji, E.; Santosh, M.; Sarath, K.V.; Prakash, P.; Deepchand, V.; Divya, B.V. Arsenic Contamination of Groundwater: A Global Synopsis with Focus on the Indian Peninsula. *Geosci. Front.* **2021**, *12*, 101079. [[CrossRef](#)]
- Chakraborty, T.K.; Chandra Ghosh, G.; Hossain, M.R.; Islam, M.S.; Habib, A.; Zaman, S.; Bosu, H.; Nice, S.; Haldar, M.; Khan, A.S. Human Health Risk and Receptor Model-Oriented Sources of Heavy Metal Pollution in Commonly Consume Vegetable and Fish Species of High Ganges River Floodplain Agro-Ecological Area, Bangladesh. *Heliyon* **2022**, *8*, e11172. [[CrossRef](#)]
- Zhang, Z.; Xiao, C.; Adeyeye, O.; Yang, W.; Liang, X. Source and Mobilization Mechanism of Iron, Manganese and Arsenic in Groundwater of Shuangliao City, Northeast China. *Water* **2020**, *12*, 534. [[CrossRef](#)]

5. Santha, N.; Sangkajan, S.; Saenton, S. Arsenic Contamination in Groundwater and Potential Health Risk in Western Lampang Basin, Northern Thailand. *Water* **2022**, *14*, 465. [CrossRef]
6. Abbaspour, N.; Hurrell, R.; Kelishadi, R. Review on Iron and Its Importance for Human Health. *J. Res. Med. Sci.* **2014**, *19*, 164–174. [PubMed]
7. Li, L.; Yang, X. The Essential Element Manganese, Oxidative Stress, and Metabolic Diseases: Links and Interactions. *Oxidative Med. Cell. Longev.* **2018**, *2018*, 7580707. [CrossRef] [PubMed]
8. Ye, Q.; Park, J.E.; Gughani, K.; Betharia, S.; Pino-Figueroa, A.; Kim, J. Influence of Iron Metabolism on Manganese Transport and Toxicity. *Metallomics* **2017**, *9*, 1028–1046. [CrossRef] [PubMed]
9. Kohgo, Y.; Ikuta, K.; Ohtake, T.; Torimoto, Y.; Kato, J. Body Iron Metabolism and Pathophysiology of Iron Overload. *Int. J. Hematol.* **2008**, *88*, 7–15. [CrossRef]
10. Avila, D.S.; Puntel, R.L.; Aschner, M. Manganese in Health and Disease. In *Interrelations between Essential Metal Ions and Human Diseases; Metal Ions in Life Sciences*; Sigel, A., Sigel, H., Sigel, R.K.O., Eds.; Springer: Dordrecht, The Netherlands, 2013; Volume 13, pp. 199–227.
11. Fatoki, J.O.; Badmus, J.A. Arsenic as an Environmental and Human Health Antagonist: A Review of Its Toxicity and Disease Initiation. *J. Hazard. Mater.* **2022**, *5*, 100052. [CrossRef]
12. WHO. Progress on Drinking Water, Sanitation and Hygiene: 2017 Update and SDG Baselines. World Health Organization (WHO), Geneva and the United Nations Children’s Fund (UNICEF), New York. Available online: <https://www.who.int/publications-detail-redirect/9789241549950> (accessed on 27 December 2022).
13. Inyang, M.I.; Gao, B.; Yao, Y.; Xue, Y.; Zimmerman, A.; Mosa, A.; Pullammanappallil, P.; Ok, Y.S.; Cao, X. A Review of Biochar as a Low-Cost Adsorbent for Aqueous Heavy Metal Removal. *Crit. Rev. Environ. Sci. Technol.* **2016**, *46*, 406–433. [CrossRef]
14. Li, H.; Dong, X.; da Silva, E.B.; de Oliveira, L.M.; Chen, Y.; Ma, L.Q. Mechanisms of Metal Sorption by Biochars: Biochar Characteristics and Modifications. *Chemosphere* **2017**, *178*, 466–478. [CrossRef]
15. Gao, N.; Du, W.; Zhang, M.; Ling, G.; Zhang, P. Chitosan-Modified Biochar: Preparation, Modifications, Mechanisms and Applications. *Int. J. Biol. Macromol.* **2022**, *209*, 31–49. [CrossRef] [PubMed]
16. Loc, N.X.; Tuyen, P.T.T.; Mai, L.C.; Phuong, D.T.M. Chitosan-Modified Biochar and Unmodified Biochar for Methyl Orange: Adsorption Characteristics and Mechanism Exploration. *Toxics* **2022**, *10*, 500. [CrossRef] [PubMed]
17. Rubeena, K.K.; Hari Prasad Reddy, P.; Lajju, A.R.; Nidheesh, P.V. Iron Impregnated Biochars as Heterogeneous Fenton Catalyst for the Degradation of Acid Red 1 Dye. *J. Environ. Manag.* **2018**, *226*, 320–328. [CrossRef] [PubMed]
18. Dalahmeh, S.S.; Stenström, Y.; Jebrane, M.; Hylander, L.D.; Daniel, G.; Heinmaa, I. Efficiency of Iron- and Calcium-Impregnated Biochar in Adsorbing Phosphate from Wastewater in Onsite Wastewater Treatment Systems. *Front. Environ. Sci.* **2020**, *8*, 538539. [CrossRef]
19. He, R.; Peng, Z.; Lyu, H.; Huang, H.; Nan, Q.; Tang, J. Synthesis and Characterization of an Iron-Impregnated Biochar for Aqueous Arsenic Removal. *Sci. Total Environ.* **2018**, *612*, 1177–1186. [CrossRef] [PubMed]
20. Fan, J.; Xu, X.; Ni, Q.; Lin, Q.; Fang, J.; Chen, Q.; Shen, X.; Lou, L. Enhanced As (V) Removal from Aqueous Solution by Biochar Prepared from Iron-Impregnated Corn Straw. *J. Chem.* **2018**, *2018*, 5137694. [CrossRef]
21. Sun, Y.; Yu, F.; Han, C.; Houda, C.; Hao, M.; Wang, Q. Research Progress on Adsorption of Arsenic from Water by Modified Biochar and Its Mechanism: A Review. *Water* **2022**, *14*, 1691. [CrossRef]
22. Khawkomol, S.; Neamchan, R.; Thongsamer, T.; Vinitnantharat, S.; Panpradit, B.; Sohsalam, P.; Werner, D.; Mroziak, W. Potential of Biochar Derived from Agricultural Residues for Sustainable Management. *Sustainability* **2021**, *13*, 8147. [CrossRef]
23. Wang, A.; Zou, D.; Zeng, X.; Chen, B.; Zheng, X.; Li, L.; Zhang, L.; Xiao, Z.; Wang, H. Speciation and Environmental Risk of Heavy Metals in Biochars Produced by Pyrolysis of Chicken Manure and Water-Washed Swine Manure. *Sci. Rep.* **2021**, *11*, 11994. [CrossRef] [PubMed]
24. Thongsamer, T.; Vinitnantharat, S.; Pinisakul, A.; Werner, D. Chitosan Impregnation of Coconut Husk Biochar Pellets Improves Their Nutrient Removal from Eutrophic Surface Water. *Sustain. Environ. Res.* **2022**, *32*, 39. [CrossRef]
25. Lamaming, J.; Saalah, S.; Rajin, M.; Ismail, N.M.; Yaser, A.Z. A Review on Bamboo as an Adsorbent for Removal of Pollutants for Wastewater Treatment. *Int. J. Chem. Eng. Res.* **2022**, *2022*, 7218759. [CrossRef]
26. Hernandez-Mena, L.; Pecora, A.; Beraldo, A. Slow Pyrolysis of Bamboo Biomass: Analysis of Biochar Properties. *Chem. Eng. Trans.* **2014**, *37*, 115–120.
27. Vinitnantharat, S.; Rattanasirisophon, W.; Ishibashi, Y. Modification of Granular Activated Carbon Surface by Chitosan Coating for Geosmin Removal: Sorption Performances. *Water Sci. Technol.* **2017**, *55*, 145–152. [CrossRef]
28. Kalaruban, M.; Loganathan, P.; Nguyen, T.V.; Nur, T.; Jahir, M.A.H.; Nguyen, T.H.; Trinh, M.V. Iron-impregnated Granular Activated Carbon for Arsenic Removal: Application to Practical Column Filters. *J. Environ. Manag.* **2019**, *239*, 235–243. [CrossRef]
29. Kashem, M.A.; Singh, B.R.; Kondo, T.; Imamul Huq, S.M.; Kawai, S. Comparison of Extractability of Cd, Cu, Pb and Zn with Sequential Extraction in Contaminated and Non-contaminated Soils. *Int. J. Environ. Sci. Tech.* **2007**, *4*, 169–176. [CrossRef]
30. Chongtham, N.; Bisht, M.S.; Santosh, O.; Bajwa, H.K.; Indira, A. Mineral Elements in Bamboo Shoots and Potential Role in Food Fortification. *J. Food Compos. Anal.* **2021**, *95*, 103662. [CrossRef]
31. Mianowski, A.; Owczarek, M.; Marecka, A. Surface Area of Activated Carbon Determined by the Iodine Adsorption Number. *Energy Sources Part A* **2007**, *29*, 839–850. [CrossRef]

32. Simoes, M.C.; Hughes, K.J.; Ingham, D.B.; Ma, L.; Pourkashanian, M. Estimation of the Thermochemical Radii and Ionic Volumes of Complex Ions. *Inorg. Chem.* **2017**, *56*, 7566–7573. [[CrossRef](#)]
33. Sahool, S.S.; Vijay, V.K.; Chandra, R.; Kumar, H. Production and Characterization of Biochar Produced from Slow Pyrolysis of Pigeon Pea Stalk and Bamboo. *J. Clean. Prod.* **2021**, *3*, 100101.
34. Chen, D.; Yu, X.; Song, C.; Pang, X.; Huang, J.; Li, Y. Effect of Pyrolysis Temperature on the Chemical Oxidation Stability of Bamboo Biochar. *Bioresour. Technol.* **2016**, *218*, 1303–1306. [[CrossRef](#)] [[PubMed](#)]
35. Spokas, K.A. Review of the Stability of Biochar in Soils: Predictability of O:C Molar Ratios. *Carbon Manag.* **2010**, *1*, 289–303. [[CrossRef](#)]
36. Kruatong, N.; Vinitnantharat, S.; Pinisakul, A.; Wilamas, A.; Sukkhe, N. Use of Biochar Impregnated with Iron and Chitosan for Heavy Metal Removal: Sorption Performances. In Proceedings of the 47th International Congress on Science, Technology and Technology-Based Innovation: Sciences for SDGs: Challenges and Solutions, Kasetsart University, Kamphaeng Saen Campus, Nakhon Pathom, Thailand, 5–7 October 2021; pp. 614–620.
37. Kirmizakis, P.; Tawabini, B.; Siddiq, O.M.; Kalderis, D.; Ntarlagiannis, D.; Soupios, P. Adsorption of Arsenic on Fe-modified Biochar and Monitoring Using Spectral Induced Polarization. *Water* **2022**, *14*, 563. [[CrossRef](#)]
38. Jiménez-Cedillo, M.J.; Olguín, M.T.; Fall, C.; Colin-Cruz, A. As(III) and As(V) Sorption on Iron-modified Non-pyrolyzed and Pyrolyzed Biomass from *Petroselinum crispum* (Parsley). *J. Environ. Manag.* **2013**, *117*, 242–252. [[CrossRef](#)]
39. Lodhi, G.; Kim, Y.S.; Hwang, J.W.; Kim, S.K.; Jeon, Y.J.; Je, J.Y.; Ahn, C.B.; Moon, S.H.; Jeon, B.T.; Park, P.J. Chitooligosaccharide and Its Derivatives: Preparation and Biological Applications. *Biomed. Res. Int.* **2014**, *2014*, 654913. [[CrossRef](#)]
40. Nomanbhay, S.M.; Palanisamy, K. Removal of Heavy Metal from Industrial Wastewater Using Chitosan Coated Oil Palm Shell Charcoal. *Electron. J. Biotechnol.* **2005**, *8*, 43–53. [[CrossRef](#)]
41. Hove, M.; van Hille, R.P.; Lewis, A.E. Mechanisms of Formation of Iron Precipitates from Ferrous Solutions at High and Low pH. *Chem. Eng. Sci.* **2008**, *63*, 1626–1635. [[CrossRef](#)]
42. Aziz, H.A.; Smith, P.G. The Influence of pH and Coarse Media on Manganese Precipitation from Water. *Wat. Res.* **1992**, *26*, 853–855. [[CrossRef](#)]
43. LIRT. Groundwater Quality Standard for Drinking Purpose, Notification of the Ministry of Industry, No. 12, BE 2542 (1999). Legislative Institutional Repository of Thailand. Available online: <https://dl.parliament.go.th/handle/20.500.13072/230880> (accessed on 27 March 2023).
44. Saikia, A.; Agnihotri, G.; Raul, K.P.; Banerjee, S.; Dwivedi, K.S. Integrated Approach to Remove Iron, Arsenic and Manganese from Water Using Manganese Greensand and Other Adsorbent. *Indian J. Environ. Sci.* **2020**, *16*, 105.
45. Naik, D.K.; Monika, K.; Prabhakar, S.; Parthasarathy, R.; Satyavathi, B. Pyrolysis of Sorghum Bagasse Biomass into Bio-char and Bio-oil Products. *J. Therm. Anal. Calorim.* **2017**, *127*, 1277–1289. [[CrossRef](#)]
46. Liang, H.; Zhu, C.; Ji, S.; Kannan, P.; Chen, F. Magnetic Fe<sub>2</sub>O<sub>3</sub>/biochar Composite Prepared in a Molten Salt Medium for Antibiotic Removal in Water. *Biochar* **2022**, *4*, 3. [[CrossRef](#)]
47. Zeng, X.; Xiao, Z.; Zhang, G.; Wang, A.; Li, Z.; Liu, Y.; Wang, H.; Zeng, Q.; Liang, Y.; Zou, D. Speciation and Bioavailability of Heavy Metals in Pyrolytic Biochar of Swine and Goat manures. *J. Anal. Appl. Anal.* **2018**, *132*, 82–93. [[CrossRef](#)]

**Disclaimer/Publisher’s Note:** The statements, opinions and data contained in all publications are solely those of the individual author(s) and contributor(s) and not of MDPI and/or the editor(s). MDPI and/or the editor(s) disclaim responsibility for any injury to people or property resulting from any ideas, methods, instructions or products referred to in the content.